# Spray penetration in a turbulent flow

Jacek Pozorski[1], Sergei Sazhin[2], Marta Goździkowska[1],

Cyril Crua[2], David Kennaird[2] and Morgan Heikal[2]

[1] *Institute of Fluid-Flow Machinery, Polish Academy of Sciences*

*ul. Fiszera 14, Gdańsk, Poland*; *e-mail: jp@imp.gda.pl*

[2] *School of Engineering, University of Brighton, Brighton BN2 4GJ,*

*United Kingdom, E-mail: S.Sazhin@brighton.ac.uk*

February 15, 2002

(manuscript, resubmitted to 'Flow, Turbulence and Combustion')

**Keywords:** two-phase flow, turbulent dispersion, spray stopping distance

**Abstract**

Analytical expressions for mass concentration of liquid fuel in a spray are derived taking into account the effects of gas turbulence, and assuming that the influence of droplets on gas is small (intitial stage of spray development). Beyond a certain distance the spray is expected to be fully dispersed. This distance is identified with the maximum spray penetration. Then the influence of turbulence on the spray stopping distance is discussed and the r.m.s. spray penetration is computed from a trajectory (Lagrangian) approach. Finally, the problem of spray penetration is investigated in a homogeneous two-phase flow regime taking into account the dispersion of spray away from its axis. It is predicted that for realistic values of spray parameters the spray penetration at large distances from the nozzle is expected to be proportional to $t^{2/3}$ (in the case when this dispersion is not taken into account this distance is proportional to $t^{1/2}$). The $t^{2/3}$ law is supported by experimental observations for a high pressure injector.

# 1 Introduction

The study of two-phase flows with a dispersed phase is an interesting and rapidly developing field of science with a variety of theoretical problems and practical applications, including agriculture, food industry, chemical and process engineering, and internal combustion engines. Fuel injection in a Diesel engine is an example of the industrial process where the dispersed phase is present in the form of small droplets.

For a sufficiently high load (mass fraction) of the dispersed phase, the dynamics of the two-phase dispersed flow needs to be described with two-way momentum coupling accounted for. This means that both particle dynamics and continuous phase (fluid) velocity have to be computed at the same time. For low dispersed phase loads, a simpler description in terms of one-way coupling is adequate. Both situations will be addressed in the paper, although two-way coupling will only be treated in a simplified fashion. It is noted that the computation of turbulent dispersed two-phase flows, both in the two-fluid and trajectory approach, remains an open area of research (see the discussion in [1, 2, 3]).

The focus of the paper is on the problem of spray penetration as one of the most important for practical application (e.g. [4, 5, 6, 7]). This problem was addressed by a number of authors (see reviews in [8, 9]), but in all studies, the spray penetration was determined either based on empirical correlations or on simplified models without taking into account the effects of flow turbulence in a self-consistent way. The aim of this paper is to readdress this problem focusing specifically on the effects of turbulence on spray penetration.

The paper starts with recalling the basic equations for spray diffusion and droplet motion (Section 2). Then three limiting cases of spray development are considered. Firstly, we consider the intial stage when the influence of gas on droplet mean velocities can be assumed

small (Section 3). Then we discuss the influence of turbulence on the statistics of droplet stopping distance (Section 4). Finally, we attempt to take into account the mutual influence of droplets and gas dynamics and calculate the spray penetration in the no-slip two-phase flow regime assuming that the dispersion of droplets follows the same law as for the initial stage and we provide an experimental support for it (Section 5).

## 2 Basic equations

As generally known (cf. [1, 10]), there are two possible approaches to two-phase flow description: Eulerian and Lagrangian. In the Eulerian approach, both phases are treated as continuous, interacting and interpenetrating fluids, and the governing transport equations are written for both phases in similar forms. In this approach, the mass conservation equation for particles (droplets) in a turbulent flow can be written in the following general form ([11]):

$$\frac{\partial C}{\partial t} = -\nabla \cdot \mathbf{F}, \tag{1}$$

where $C$ is the mean mass concentration of the droplets and $\mathbf{F} = \mathbf{V}C + \mathbf{F}_t$ is the mean particle flux which arises from the motion in the main flow direction and turbulent diffusion modelled with the gradient hypothesis

$$\mathbf{F}_t = \overline{\mathbf{v}'c'} = -D_t \nabla C \ ; \tag{2}$$

$\mathbf{V}$ is the mean droplet velocity. It will be assumed that the process is steady-state ($\partial/\partial t = 0$), and the turbulent diffusivity coefficient $D_t$ is taken as a constant scalar. In this case Eq. (1)

simplifies to:

$$\nabla \cdot (\mathbf{V}C) = D_t \left( \frac{\partial^2 C}{\partial x^2} + \frac{\partial^2 C}{\partial y^2} + \frac{\partial^2 C}{\partial z^2} \right). \tag{3}$$

On the other hand, in the Lagrangian approach the dispersed phase is treated as a set of individual inclusions; for an ample discussion of the approach and the related probability density function (PDF) description of turbulent two-phase flows, see [12]. Under simplifying assumptions, usually agreed for the case of heavy particles in a gas, the motion of an individual spherical droplet is governed by the following equation ([13]):

$$\frac{d\mathbf{V}}{dt} = \frac{3}{8 r_d} C_d \frac{\rho_g}{\rho_d} (\mathbf{U} - \mathbf{V}) |\mathbf{U} - \mathbf{V}|, \tag{4}$$

where $r_d$ and $\rho_d$ are droplet radius and density, respectively; $\rho_g$ and $\mathbf{U}$ stand for gas density and velocity. $C_d$ is the drag coefficient that depends on the Reynolds number. Following [8], $C_d$ can be approximated as:

$$C_d = \begin{cases} 24/\mathrm{Re} & \text{for Stokes regime } (\mathrm{Re} < 0.2) \\ 18.5/\mathrm{Re}^{0.6} & \text{for Allen regime } (0.2 < \mathrm{Re} < 500) \\ 0.44 & \text{for Newton regime } (500 < Re < 10^5) \end{cases} \tag{5}$$

where $\mathrm{Re} = 2|\mathbf{U} - \mathbf{V}| r_d / \nu_g$ is the Reynolds number of the relative fluid-particle motion and $\nu_g$ is the gas kinematic viscosity.

Equation (4) describes the slowing down of droplets due to the aerodynamic drag force. If the two-way momentum coupling is accounted for, gas is accelerated at the same time in order to satisfy global momentum conservation.

Equation (4) is formulated for mean velocities in turbulent flow and and gives only mean particle displacements. The description of the turbulent diffusion (dispersion) of droplets needs to be based on instantaneous gas velocities (cf. [14]). This means that the fluctuating

velocities of gas, removed during the Reynolds averaging, have to be accounted for. This can be done either through the turbulent diffusion coefficient in the two-fluid formalism, see Equation (2), or through the random-walk methods in the trajectory approach (cf. [15]). The next section will address the issue of the turbulent dispersion from the Eulerian standpoint, with the emphasis put on analytically integrable solutions of Equation (3) rather than on the evaluation of turbulent transport coefficients. Then the Lagrangian approach will be pursued.

# 3 Turbulent dispersion at the initial stage of spray development

The problem of spray penetration at the inital stage of spray development (close to the injector), taking into account the entrainment of air, but not the effects of turbulence has been considered in [8]. It has been shown that the spray penetration can be estimated by the following general formulae:

$$z = V_0 t - 0.5 V_0 \alpha t^2 + \tfrac{4}{15} \alpha \kappa \sqrt{V_0} t^{5/2} \qquad \text{Stokes regime} \tag{6}$$

$$z = V_0 t - 0.5 V_0^{1.4} \beta t^2 + 0.373 \kappa V_0^{0.9} \beta t^{5/2} \qquad \text{Allen regime} \tag{7}$$

$$z = V_0 t - 0.5 V_0^2 \gamma t^2 + 0.533 \gamma \kappa V_0^{3/2} t^{5/2} \qquad \text{Newton regime} \tag{8}$$

where $V_0$ is the initial spray injection velocity and the parameters $\alpha$, $\beta$, $\gamma$ and $\kappa$ do not depend on $z$ or $t$ (expressions for them are given in [8]).

The effects of air entrainment (together with the identification of main spray zones) are thoroughly discussed in [16]. However, for the sake of simplicity we ignore them here, omitting

last terms in the right hand sides of Equations (6)–(8). Assuming that the first terms in the right hand sides of all three equations dominate over the second terms, we can present these equations in the following compact form:

$$V = V_0 - \alpha_0 z, \tag{9}$$

where $V = dz/dt$, $\alpha_0 = \alpha$ for the Stokes flow, $\alpha_0 = V_0^{0.4}\beta$ for the Allen flow, and $\alpha_0 = V_0\gamma$ for the Newton flow; $\alpha_0$ can be interpreted as inverse to the particle aerodynamic relaxation time $\tau_p$. Note that Equation (9) is valid when

$$z \ll V_0/\alpha_0. \tag{10}$$

Having substituted Equation (9) into Equation (3) and assuming that diffusion in the main flow direction can be ignored, one obtains the following equation for mean mass concentration of droplets:

$$(V_0 - \alpha_0 z)\frac{\partial C}{\partial z} = D_t\left(\frac{\partial^2 C}{\partial x^2} + \frac{\partial^2 C}{\partial y^2}\right) + \alpha_0 C\ . \tag{11}$$

The $\alpha_0 C$ term represents a source for Equation (11): the slow-down of droplets increases their concentration in a control volume. Using the Fourier transform method and taking the boundary condition $C(x, y, 0) \propto \delta(x)\delta(y)$ where $\delta$ is the Dirac delta function, the solution of Equation (11) can be written as:

$$C(x, y, z) = \frac{\dot{m}}{4\pi V_0 D_t t}\exp\left(-\frac{x^2 + y^2}{4D_t t}\right)\exp(\alpha_0 t) \tag{12}$$

where there is a one-to-one correspondence between time and the streamwise coordinate $z$, resulting from the integration of (9)

$$t = -\frac{1}{\alpha_0}\ln\left(1 - \frac{\alpha_0 z}{V_0}\right)\ ;$$

$\dot{m}$ is the mass flow rate:

$$\dot{m} = V(z) \iint_{-\infty}^{\infty} C(x, y, z)\, dx\, dy = \text{const.} \tag{13}$$

In view of condition (10) we can simplify the expression for $t$ to: $t = z/V_0 + \alpha_0 z^2/2V_0^2$. This allows us to rewrite Equation (12) as

$$C(x, y, z) = \frac{\dot{m}\left(1 + \frac{\alpha_0 z}{2V_0}\right)}{4\pi D_t z} \exp\left[-\frac{V_0 r^2}{4D_t z}\left(1 - \frac{\alpha_0 z}{2V_0}\right)\right] \tag{14}$$

where $r = \sqrt{x^2 + y^2}$; when deriving Equation (14), higher-order terms in $z$ have been ignored. In the zeroth-order approximation, the above simplifies to:

$$C(x, y, z) = \frac{\dot{m}}{4\pi D_t z} \exp\left[-\frac{V_0 r^2}{4D_t z}\right] \ . \tag{15}$$

Let us now assume that a measuring instrument detects concentration values greater than a certain threshold $C_{\text{cut}}$. This is indeed the case of spray snapshots taken with a fast camera [9]. In this case, from (15) where $C(x, y, z) = C_{\text{cut}} = \text{const}$, the spray boundary can be found; it can conveniently be presented as:

$$r = \sqrt{\frac{-4D_t z \ln(a_s z)}{V_0}} \tag{16}$$

where $a_s = 4\pi D_t C_{\text{cut}}/\dot{m}$. As follows from Equation (16), the maximum possible spray penetration is determined from the condition $\ln(a_s z) < 0$ or:

$$z = 1/a_s \equiv \frac{\dot{m}}{4\pi D_t C_{\text{cut}}}. \tag{17}$$

Beyond the distance defined by Equation (17) the spray is expected to be fully dispersed by the turbulence and cannot be detected. However, in most practical cases the assumption (10), on which our analysis was based, is expected to be no longer valid unless the level of

turbulence is high enough ($D_t$ is large), fuel mass flow rate $\dot{m}$ is low, or the level of spray detection $C_{\rm cut}$ is high. In view of (11) the range of applicability of Eq (19) can be presented as:

$$\frac{\dot{m}}{4\pi D_t C_{\rm cut}} \ll \frac{V_0}{\alpha_0}.$$

In the case of the Stokes flow this condition can be presented in a more explicit way:

$$\frac{\dot{m}}{4\pi D_t C_{\rm cut}} \ll \frac{2V_0 r_d \rho_d}{9\mu_g}.$$

This inequality is always satisfied when the mass flow rate is small enough. We found it difficult to provide more specific estimates for $\dot{m}$ due to uncertainty of the value of $C_{\rm cut}$. The range of validity of the initial stage approximation and the transition from the initial stage to no-slip two-phase flow was discussed in detail in our previous paper [8].

# 4 Spray stopping distance in a turbulent flow

**Statistical considerations.** Here, an alternative approach to the problem of spray penetration based on the Lagrangian calculation of spray stopping distance is considered. We assume one-way momentum coupling (no gas entrainment due to droplet motion) which enables to avoid the computation of the flow (continuous phase) dynamics. We assume the homogeneous isotropic turbulence of zero mean velocity in the spray area (e.g. the combustion chamber in internal combustion engines at the end of compression stroke). Previously essential limitations such as $V = V(z)$, $\partial^2 C/\partial z^2 = 0$ are now relaxed. Unsteady phenomena due to finite injection time and droplets polydispersity can readily be simulated.

To account for turbulent dispersion the particle equation of motion has been written for droplet velocities $\mathbf{v} = \mathbf{V} + \mathbf{v}'$ (cf. Equation (4)): and instantaneous flow velocity $\mathbf{u} = \mathbf{U} + \mathbf{u}'$

(as seen by the dispersed phase)

$$\frac{d\mathbf{x}}{dt} = \mathbf{v} \tag{18}$$

$$\frac{d\mathbf{v}}{dt} = \frac{\mathbf{u}(\mathbf{x},t)-\mathbf{v}}{\tau_p}, \tag{19}$$

where the fluctuating flow velocity $\mathbf{u}'$ has to be reconstructed from known turbulence characteristics: its kinetic energy $k$ or velocity scale $\sigma_u = (2k/3)^{1/2}$ and the integral Lagrangian time scale $T_L$. Analysis has been based on the Langevin equation as a model for fluid turbulent velocity (cf. [17]); here, it also serves to model the fluid dynamics along droplet trajectories (cf. [14]). Its simplest form writes

$$d\mathbf{u}' = -\frac{\mathbf{u}'}{T_L}\,dt + \sigma_u\sqrt{2/T_L}\,d\mathbf{W} \tag{20}$$

where $d\mathbf{W}$ stands for the increment of the Wiener process. The Langevin equation is the starting point for one-point probability density function (PDF) approach in turbulence modelling. This equation has been modified to account for heavy particle dispersion ([18]) with account of gravity and particle inertia effects. Monte Carlo simulations yield the mean concentration field $C(r,z)$, as the ensemble average over a certain number of droplet trajectories. As illustrated below, turbulent character of the underlying fluid flow affects the spray dynamics including spray penetration statistics.

The modifications to the spray stopping distance (penetration) due to turbulence can be estimated via computation of the mean value $\langle z\rangle$ and variance $\langle (z-\langle z\rangle)^2\rangle$ of $z(t)$ using a given temporal correlation of the turbulent field and applying the PDF formalism for dispersed two-phase flows ( cf. [14]).

Using the governing system of Equations (18)–(20) in the 1D setting, we computed the spray stopping distance defined as $z_{stop} = z(t_\infty)$; in practice, the integration was performed up

to $t_\infty = 10\tau_p$. Spray particle motion was simulated in the homogeneous isotropic turbulence described by the fluctuating velocity scale $\sigma_u$ and the Lagrangian autocorrelation time scale $T_L$. As follows from Equation (19) averaged over realisations of fluid turbulent velocity, in the one-point statistical description the mean particle velocity $V(t)$ is not affected by turbulence. The same holds for the mean stopping distance $\langle z_{stop} \rangle = V_0 \tau_p$ where $V_0$ is the initial particle velocity.

In Fig. 1, several particle trajectories and velocity records are plotted for moderate relative turbulence intensity $\sigma_u/V_0$ to make the fluctuations clearly seen; they are compared with the deterministic case of $\sigma_u = 0$ (or the mean record). As follows from the figure, the particle stopping distance in a turbulent flow can be defined in the statistical sense only (as the individual particles do not actually stop). Moreover, the diffusive character of motion becomes dominant at later times. Next, we computed the particle coordinates at $t/\tau_p = 10$ arbitrarily defined as the stopping time. The rms of particle coordinate at that time is non-dimensionalised by the reference length $z_{ref}$ chosen as the deterministic stopping distance $z_{ref} = z_{stop}(\sigma_u = 0)$. Numerical results for two different values of the Stokes number are presented in Fig. 2. It is readily seen that the rms decreases with particle inertia and increases with the turbulence intensity.

Yet, the analysis presented above has a serious limitation, for it neglects gas entrainment due to droplet motion. A more realistic model based on the no-slip two-phase flow approximation with a two-way momentum coupling is discussed in the next section.

**Effect of turbulent structures.** Particles (droplets) correlate with certain instantaneous structures of the turbulent velocity field when the Stokes number $\mathrm{St} = \tau_p/T_L = \mathcal{O}(1)$; this

leads to the effect of preferential concentrations ([19]). As a result, for particles moving in an external field (gravity), their final settling velocity in turbulent fluid (but with zero mean velocity) differs from that measured in a stagnant fluid ([20, 21]). The settling velocity can be considerably larger, depending on St. This effect has been first observed in a laminar cellular flow field ([22]) and in random turbulence simulations ([23, 24]). We argue now that in the case of spray injection into a turbulent gas (without gravity effects), the same physical mechanisms will lead to the increase of the spray stopping distance, especially due to the particle-structures interaction in the second phase of their motion when particles have considerably slowed down.

# 5 No-slip two-phase flow

**Theoretical analysis.** In the recent paper [8] analytical expressions for spray penetration were derived based on equations for conservation of mass and momentum for a two phase flow. A number of simplifying assumptions were made when deriving these equations. Namely, it was assumed that the density of mixture of gas and droplets in the planes perperdicular to spray axis remains constant inside the spray and zero outside it. The shape of the spray boundary was controlled exclusively by the spray cone angle. In what follows we suggest an approach similar to that discussed in [8], but these two assumptions will now be relaxed.

Instead of assuming that the density of mixture of spray and droplets ($\rho_m$) is constant in the planes perpendicular to spray axis inside the spray, we assume that it depends on the distance from the spray axis $r$ in the same way as at the initial stage, see Equation (15).

This allows us to write the equation for $\rho_m$ in the form:

$$\rho_m = \rho_{m0}(z) \exp\left[-\frac{V_0 r^2}{4 D_t z}\right], \tag{21}$$

where $\rho_{m0}(z)$ is the mixture density at the axis of the spray; the form of this function does not need to be specified at this stage.

Assuming that $\rho_{m0}(z)$ is a weak function of $z$, Equation (21) predicts that the curves of constant $\rho_m$ correspond to $r \propto \sqrt{z}$. This parabolic form of the spray shape was observed in the experiments [9]. Assuming axial symmetry of the spray and supposing that the velocity of the mixture $v_m$ is constant for given $z$, we calculate the mass flow rate of the mixture of droplets and gas at the level $z$ as

$$\dot{m} = 2\pi \int_0^\infty v_m \rho_m r \, \mathrm{d}r = \frac{4\pi D_t \rho_{m0} v_m z}{V_0} = \rho_{m0} A_m v_m \tag{22}$$

where $A_m = 4\pi D_t z / V_0$ is the effective cross-section of the spray.

Equation (22) predicts that the mass flow rate is zero when $z \to 0$. This means that this equation cannot be applied for those $z$ where the intial stage approximation is valid. At the same time one would be interested in constructing a model which could predict accurate results for large $z$, but still reasonable ones for $z \to 0$. This can be achieved by replacing the effective cross-section introduced above by $A_m$ defined as:

$$A_m = A_0 + 4\pi D_t z / V_0, \tag{23}$$

where $A_0$ is the cross-sectional area of the nozzle. In the limit $z \to \infty$ the contribution of $A_0$ is expected to be negligibly small, while in the limit $z \to 0$ Equation (23) reduces to a physically correct statement that $A_m = A_0$.

Ignoring the contribution of air outside of the area $A_m$ and assuming that the relative volume concentration of droplets $\alpha_d$ is small (this assumption is valid everywhere except the

immediate vicinity of the nozzle), we can write the equation of conservation of mass in the form almost identical to the corresponding equation used in [8] (see their Equation (27)):

$$\rho_d A_0 V_0 = \rho_{m0} A_m v_m - (1-\alpha_d) A_m \rho_g v_m, \tag{24}$$

where $A_m$ is defined by Eq (23), $\alpha_d$ is the volume fraction of droplets (assumed to be small).

In a similar way we can write the equation for conservation of momentum in the form (cf. Equation (29) of [8]):

$$\rho_d A_0 V_0^2 = \rho_{m0} A_m v_m^2. \tag{25}$$

The combination of Equations (23), (24) and (25) gives us the following equation of the velocity of the mixture (cf. a similar analysis in [8]):

$$v_m \equiv \frac{\mathrm{d}z}{\mathrm{d}t}_{|m} = \frac{2V_0}{1+\sqrt{a+bz}}, \tag{26}$$

where

$$a = 1 + 4(1-\alpha_d)\tilde{\rho_a}; \qquad b = \frac{64(1-\alpha_d)D_t\tilde{\rho_a}}{V_0 d_0^2}; \qquad \tilde{\rho_a} = \rho_g/\rho_d,$$

$d_0$ is the diameter of the injector. Integration of Equation (26) gives:

$$3bz + 2(a+bz)^{3/2} = 6V_0 bt. \tag{27}$$

For sufficiently large $z$ we can assume that $bz \gg a$ and simplify Equation (27) to

$$z = \left(\frac{9V_0^2}{b}\right)^{1/3} t^{2/3} = \frac{V_0}{4}\left(\frac{9d_0^2}{(1-\alpha_d)\tilde{\rho}_a D_t}\right)^{1/3} t^{2/3}\ . \tag{28}$$

The dependence of $z$ can be compared with the one predicted in [8] in the limit $t \to \infty$:

$$z = \frac{\sqrt{V_0 d_0 t}}{(1-\alpha_d)^{1/4}\tilde{\rho}_a^{1/4}\sqrt{\tan\theta}}, \tag{29}$$

where $\theta$ is the spray half-cone angle assumed to be constant. In the limit $\alpha_d \to 0$ Equations (28) and (29) predict the same penetration if:

$$D_t = \frac{9}{64} \frac{V_0^{3/2} (\tan\theta)^{3/2} \sqrt{d_0 t}}{\tilde{\rho}_a^{1/4}} \,. \tag{30}$$

Considering the values of parameters for experimental results discussed in [8] (case 1): $V_0 = 318.3$ m/s, $d_0 = 0.2$ mm, $\theta = 13^\circ$, $t = 1$ ms, $\tilde{\rho}_a = 19.7/760 = 0.025$, we obtain $D_t = 0.1$ m$^2/s$. Tentatively, the turbulent diffusivity coefficient can be roughly estimated from the Tchen formula $D_t = \sigma_u^2 T_L^*$ (strictly valid only in homogeneous turbulence for a long time limit). Then the values of $\sigma_u^2 = 2k/3$ and $T_L = \mathcal{O}(k/\epsilon)$, if experimentally available, can be used for a cross-check of the above number.

**Experimental results.** There is much uncertainty regarding the experimental observations of spray penetration as discussed in [9, 25]. The general conclusion inferred in [9] is that in the case of low pressure injection sprays the shape of the spray is close to conical and spray penetration is approximately proportional to $\sqrt{t}$. For the high pressure injection, the shape of the spray is close to parabolic, described by Equation (21). In this case we would expect that spray penetration is fairly well described by Equation (28) and proportional to $t^{2/3}$. We have checked this conclusion using data from a high-speed video recording of a Diesel spray injected at 100 MPa into air with density of 49 kg/m$^3$. The results of experimental measurements of spray penetration and the best fits of experimental data by the curves $\propto t^{1/2}$ (dashed) and $\propto t^{2/3}$ (solid) are shown in Figure 3. The experimental uncertainty of measurements was about $\pm 6\%$. As follows from this figure, the $t^{2/3}$ plot provides a noticeably better fit. The maximum and mean deviations for the plot $\propto t^{2/3}$ (37.8% and 9.6%) were clearly less than the maximum and mean deviations for the plot $\propto t^{1/2}$ (65.0% and 21.1%). This

supports our approach to explaining of spray penetration by turbulent dispersion of droplets, although more studies in this direction are needed.

# 6 Conclusions

In the theoretical analysis and numerical computations presented in the paper, a one-way momentum coupling has been assumed first. We considered the effect of fluid turbulence on droplets to derive analytical expressions for mass concentration of liquid fuel in a spray. Theoretical predictions suggest that beyond a certain distance the spray is expected to be fully dispersed in a sense that its mass concentration becomes less than the experimentally detectable threshold value. This distance has been identified with the maximum spray penetration, and the analytical expression derived for this distance is always valid when the droplet mass flow rate is sufficienly low. Then, it is pointed out that the influence of instantaneous turbulence structures can lead to a noticeable modification of the spray stopping distance itself which needs to be accounted for in practical applications. In order to estimate the r.m.s. of the spray stopping distance, we have performed a numerical Monte Carlo simulation with the use of model Langevin equation for fluid fluctuating velocity. The Lagrangian approach is seen as a complementary one, for the r.m.s. stopping distance is not available from the mean field Eulerian closures. Finally, the problem of spray penetration is investigated in a two-phase flow regime (i.e. mixture with no interphase slip velocity) taking into account the dispersion of spray away from its axis. It is predicted that for realistic values of spray parameters the spray penetration at large distances from the nozzle is expected to be proportional to $t^{2/3}$ (in the case when this dispersion is not taken into account this distance

is proportional to $t^{1/2}$). This law, supported by some available experimental data, together with the estimation of the r.m.s. stopping distance, as predicted by a Lagrangian turbulence model, is hopefully of practical interest for spray modelling.

# References


[1] Crowe, C.T. Review – Numerical Models for Dilute Gas-Particle Flows. *ASME J. Fluids Engng* **104** (1982), 297–303.

[2] Crowe, C.T., On models for turbulence modulation in fluid-particle flows. *Int. J. Multiphase Flow* **26** (2000), 719–727.

[3] Stock, D.E., Particle dispersion in flowing gases. *ASME J. Fluids Engng* **118** (1996), 4–17.

[4] Lefebvre, A., *Atomization and Sprays*, Taylor and Francis (1989).

[5] Fuel Spray Studies (eds. R. Rietz and R. Krieger), Published by Society of Automotive Engineers (1997).

[6] Siebers, D.L., Liquid-phase fuel penetration in Diesel sprays. *SAE technical report* 980809 (1998).

[7] Siebers, D.L., Scaling liquid-phase fuel penetration in Diesel sprays based on mixing-limited vaporization. *SAE technical report* 1999-01-0528 (1999).

[8] Sazhin, S.S., Feng, G. & Heikal, M.R., A model for spray penetration. *Fuel* **80**(15), 2171–2180 (2001).

[9] Savich, S., *Spray Dynamics and In-cylinder Air Motion.* PhD Thesis, The University of Brighton (2001).

[10] Simonin, O., Deutsch, E. & Minier, J.-P., Eulerian prediction of the fluid/particle correlated motion in turbulent two-phase flows. *Appl. Sci. Res.* **51** (1993), 275–283.

[11] Csanady G.T., *Turbulent diffusion in the environment*, D. Reidel Publishing Comp., Dordrecht-Holland (1973).

[12] Minier, J.-P. & Peirano, E., The PDF approach to turbulent polydispersed two-phase flows. *Phys. Rep.* **352** (2001), 1–214.

[13] Maxey, M.R. & Riley, J.J., Equation of motion for a small rigid sphere in a nonuniform flow. *Phys. Fluids* **26** (1983), 883–889.

[14] Pozorski, J. & Minier, J.-P., PDF modeling of dispersed two-phase turbulent flows. *Phys. Rev. E* **59** (1999), 855–863.

[15] Pozorski, J., Numerical simulation of dispersed phase motion in turbulent two-phase flow. *Doctoral thesis* (1995), Institute of Fluid-Flow Machinery, Polish Academy of Sciences, Gdańsk.

[16] Ghosh, S. & Hunt, J.C.R., Induced air velocity within droplet driven sprays. *Proc. R. Soc. Lond. A* **444** (1994), 105–127.

[17] Pope, S.B., Lagrangian PDF methods for turbulent flows. *Annu. Rev. Fluid Mech.* **26** (1994), 23–63.

[18] Pozorski, J. & Minier, J-P., On the Lagrangian turbulent dispersion models based on the Langevin equation. *Int. J. Multiphase Flow* **24** (1998), 913–945.

[19] Eaton, J.K. & Fessler, J.R., Preferential concentration of particles by turbulence. *Int. J. Multiphase Flow* **20** (1994), 169–209.

[20] Hainaux, F., Aliseda, A., Cartellier, A. & Lasheras, J.C., Settling velocity and clustering of particles in an homogeneous and isotropic turbulence. *Advances in Turbulence VIII*, Ed.: Dopazo, C. (2000), 553–556.

[21] Dávila, J. & Hunt, J.C.R., Settling of small particles near vortices and in turbulence. *J. Fluid Mech.* **440** (2001), 117–145.

[22] Maxey, M.R., The motion of small spherical particles in a cellular flow field. *Phys. Fluids* **30** (1987), 1915–1928.

[23] Maxey, M.R., The gravitational settling of aerosol particles in homogeneous turbulence and random flow fields. *J. Fluid Mech.* **174** (1987), 441–465.

[24] Wang, L.P. & Maxey, M.R., Settling velocity and concentration distribution of heavy particles in homogeneous isotropic turbulence. *J. Fluid Mech.* **256** (1993), 27–68.

[25] Naber, J.D. & Siebers, D.L., Effects of gas density and vaporization on penetration and dispersion of diesel sprays. *SAE Report* 960034 (1996).

# Figure captions:

Figure 1: Some trajectories of spray particles (left plot) and corresponding velocity records (right plots). Solid lines: three different realisations for $\sigma_u/V_0 = 0.2$ and $T_L/\tau_p = 0.2$; dashed lines: universal deterministic curve for $\sigma_u/V_0 = 0$.

Figure 2: RMS of the spray stopping distance in isotropic turbulence.

Line with $\circ$: $St = \tau_p/T_L = 1$; line with $\square$: $St = 10^2$.

Figure 3: Spray penetration versus time for injection pressure of 100 MPa and air density 49 kg/m$^3$: $\diamond$ – experimental results; - - - - approximation of experimental results by the curve $\propto t^{1/2}$; — approximation by $t^{2/3}$.

# Figures:

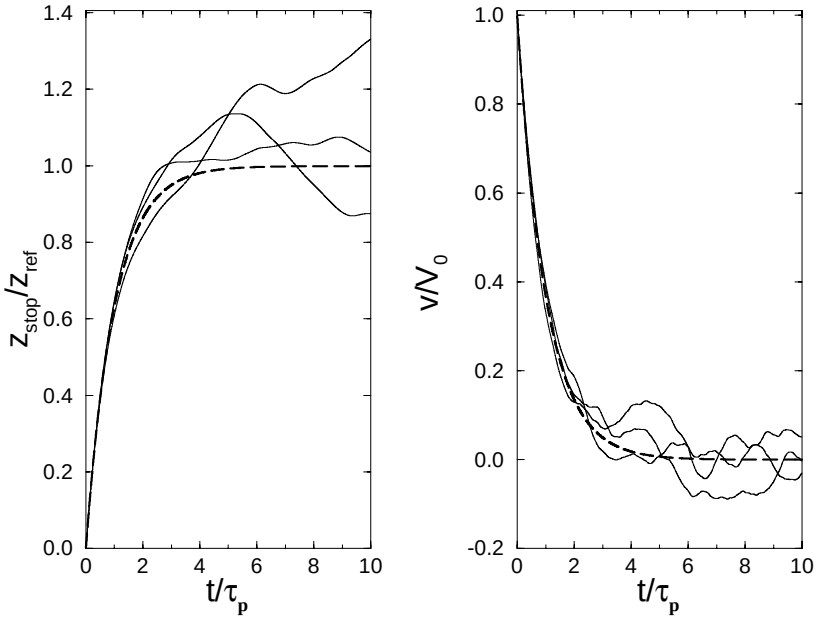


Figure 1

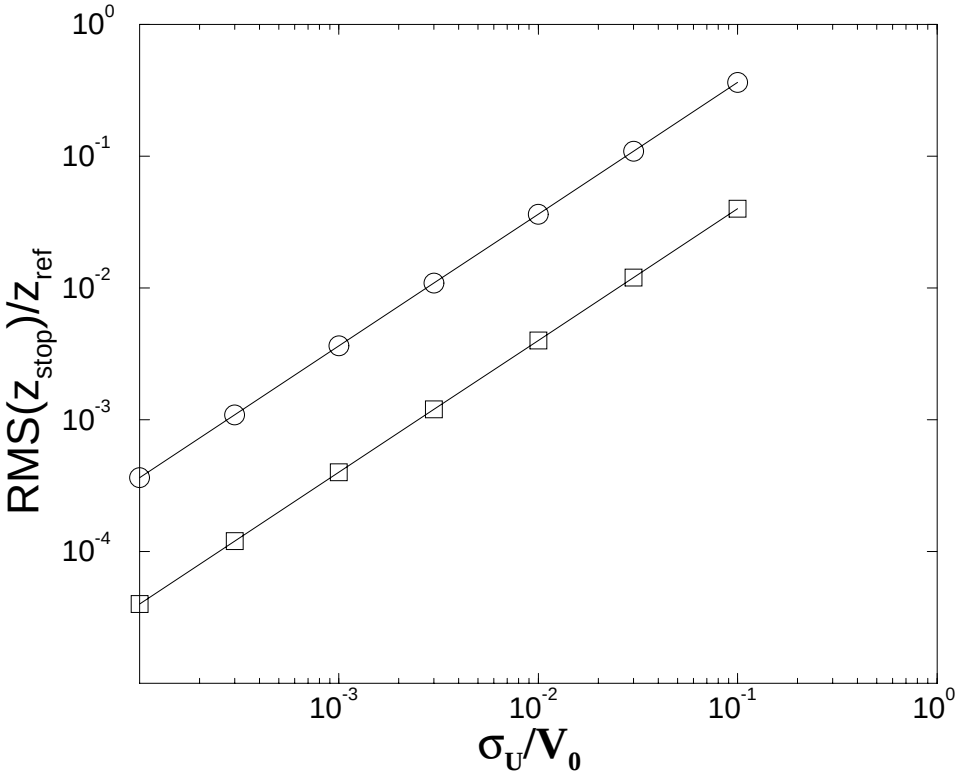


Figure 2

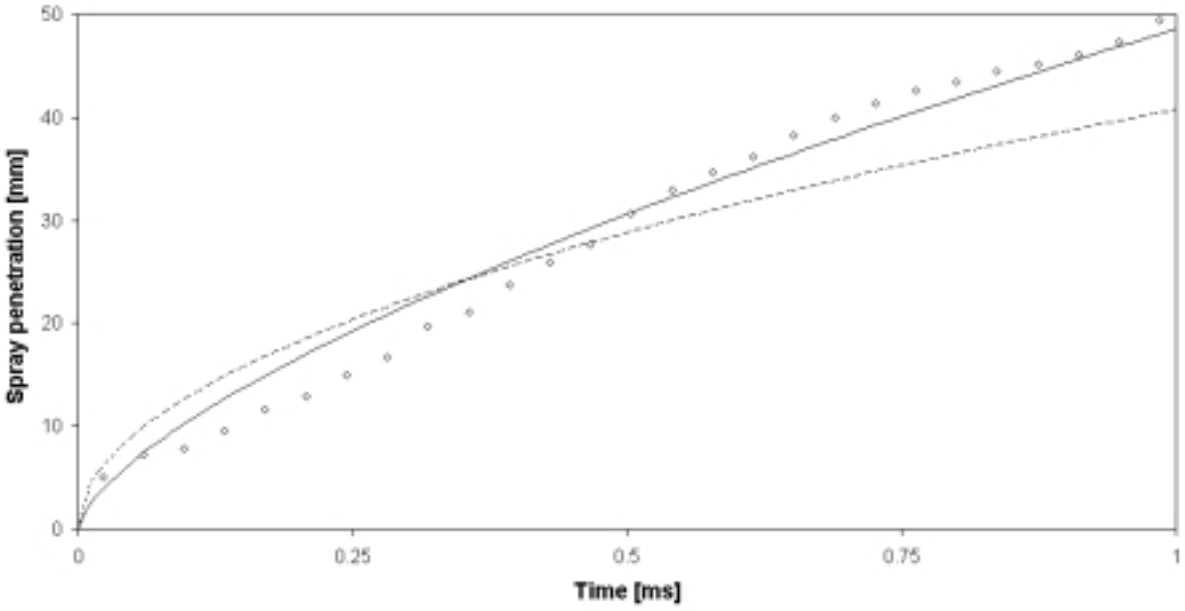


Figure 3